JOURNAL OF MATERIALS SCIENCE **37** (2002) 5291 – 5298

Analysis of the recrystallization and grain growth processes in AISI 316 stainless steel

A. DI SCHINO, J. M. KENNY
Materials Engineering Center, University of Perugia, Loc. Pentima bassa 21, 05100 Terni, Italy
E-mail: kenny@unipg.it

G. ABBRUZZESE
Centro Sviluppo Materiali, Viale Brin, 05100 Terni, Italy

A theoretical and experimental study on the recrystallization and grain growth processes on AISI 316 stainless steel is here reported. Experimental data are analyzed according to a mathematical model based on statistical assumptions able to describe simultaneously recrystallization and grain growth in metals. Taking into account the classical constitutive equations of the Taylor's theory, the model adopts two parameters: the dislocation density and the initial number of nuclei. The predictions of the model are in good agreement with experimental results. As cross check of the model predictions, the independent parameter "dislocation density" is found to properly correlate to the mechanical properties of the steel, to X-ray diffraction measurements and to transmission electron microscopy measurements. A comparison with an analogue study on AISI 304 stainless steel is also reported, enhancing the effect of molybdenum in inhibiting recrystallization and grain growth.

1. Introduction

It is well known that the mechanical properties of austenitic stainless steels are strongly affected by microstructural features (such as grain size and δ-ferrite content) and chemical composition variations (which produce solid-solution hardening by both substitutional and interstitial solid solution). There have been recent industrial developments both from the point of view of composition variations [1] and grain size [2] in order to exploit the effect of these variables to improve the mechanical properties of steel. It is then evident how both phenomena, recrystallization and grain growth, are relevant to the mechanical properties of steel, thus suggesting the necessity of mathematical models able to predict the microstructural evolution after thermomechanical cycles.

Although a significant amount of metallurgical research has already been performed in this field [3], there is still a lack of specific information on the relationships between the processing variables and material parameters characteristic of the microstructural evolution of steels. Then, the objective of the research reported here is to approach the transformations of stainless steels during thermal treatments following cold rolling, through the development and application of a mathematical model, able in general to describe the primary recrystallization and grain growth in metals. The model offers significant improvements from the original approach [4] and will be here applied to the study of these phenomena in an AISI 316 austenitic stainless steel. The model reported here could constitute the basis of an integrated approach that can be applied to better define the transformation cycles and optimise the final properties of steel.

2. Outline of the statistical model

The driving force of primary recrystallization in metals is mainly related to the reduction of the deformation energy (dislocations) introduced by cold working. Heat treatment activates the movement of dislocations and subgrain boundaries allowing the release of the deformation energy and thus restoring a "dislocation free" microstructure. Under further heat treatment, grain growth activated by boundary energy reduction is the dominant process. There have been several attempts to simulate primary recrystallization (e.g., [5]) or grain growth after primary recrystallization (e.g., [6]). Although there is a large number of existing models, they are not sophisticated enough to deal with the simultaneous and concurrent recrystallization and grain growth phenomena. In the study reported here, a mathematical model that describes simultaneously the primary recrystallization and grain growth phenomena is applied. In this approach, recrystallization nuclei are considered pre-existing and homogeneously distributed in the deformed microstructure. This assumption agrees with the classical theory of nucleation which, in the case of a "phase transformation" deformed matrix-recrystallized matrix, predicts a critical radius of the order of 10–30 nm, smaller than subgrains typically already present in a deformed metal. This approach is only qualitatively comparable with the Avrami model, which is valid for isothermal conditions and has a more

heuristic character: in this framework it corresponds to the case in which the nucleation rate is zero [7]. The statistical model, based on the assumptions of superposition of average grain curvatures of homogeneous surroundings and of a random array of the grains, leads to the following form of the grain growth rate equation [8, 9]:

$$\frac{\mathrm{d}R_i}{\mathrm{d}t} = M \sum_j \left(\frac{1}{R_j} - \frac{1}{R_i} \right) p_j \quad \text{with} \quad p_j = \frac{n_j R_j^2}{\sum\limits_j n_j R_j^2} \tag{1}$$

To describe the recrystallization process integrated with the grain growth, it is necessary to propose an extended growth equation that enables to contemporarily and continuously analyse the evolution of free nuclei in the matrix passing through partially impinged grains up to full contact. For recrystallization a nucleus must have the following characteristics [3]:

- It must be more perfect than its neighbours; that is, it must contain fewer dislocations and thereby a lower strain energy.
- The boundaries of the subgrain must be mobile by virtue of sufficient lattice misorientation between the subgrain and its neighbours. Sufficient misorientation might be about 15°, referred to a common axis of rotation.
- It must be large enough so that the additional interfacial energy that must be supplied for growth is less than the volume free energy released when a strain-free subgrain replaces strained cells.

In our approach recrystallization nuclei (sub-grains) are considered pre-existing in the deformed microstructure and characterised by their size distribution. Moreover, the grains are assumed to be all activated from the beginning and freely growing in the deformed matrix until they get in contact to each other. This process is characterised by a gradual transition from a deformation gradient activated growth, to a proper grain growth process activated by only boundary energy reduction.

The final equation for recrystallization and grain growth can therefore be written as:

$$\frac{\mathrm{d}R_i}{\mathrm{d}t} = m \left[\left(\frac{Gb^2}{3} \Delta\rho - \frac{2\gamma}{R_i} \right) \sum_{j=1}^{i^*-1} p_j + \gamma \sum_{j=i^*}^{n_c} p_j \left(\frac{1}{R_j} - \frac{1}{R_i} \right) \right] \tag{2}$$

where G is the shear modulus of the material, b is the Burger vector, ρ is the dislocation density, $\Delta\rho = \rho_d - \rho_r$ is the difference between the dislocation densities in the deformed and in the recrystallized material. In Equation 2 it is assumed that the grain boundary mobility and the surface energy of the freely growing grains in the deformed matrix are the same of those of grains in contact; i^* is the minimum class index of grains in contact with grains "i".

The main innovations in the model reported in this paper with respect to our previous approach [4], are in the calculation of the "i^*" index and in the reduction of the free calculation parameters. In particular, differently from our previous approach, in which a unique mean influence volume $V_i = \frac{1-F_V}{N}$ (where F_V is the recrystallized volume fraction and N the initial number of nuclei) was considered for all the classes, the criterion for identifying the critical class i^*, is here obtained by defining an interaction volume for each class calculated as a difference between an influence volume and the grain volume. The influence volume is here assumed proportional to the grain volume. Therefore, the final expression for the interaction volume is:

$$V_i^{\mathrm{int}} = \frac{4}{3}\pi \cdot \frac{1 - F_V}{F_V} R_i^3 = \frac{4}{3}\pi \cdot \frac{R_i^3}{F_V} - \frac{4}{3}\pi R_i^3 \tag{3}$$

where F_V is the recrystallized volume fraction. In this approach, accordingly to Equation 3, the greater is the radius R_i, the smaller is the interaction volume V_i^{int} (and thus the higher is its interaction probability). Furthermore, for $F_V = 1$ it follows that $V_i^{\mathrm{int}} = 0$, so that all the grains are in full contact.

Furthermore, in order to reduce the number of free parameters, the following constitutive equation of plastic deformation, linking the deformation ε, the dislocation density ρ, the Burger vector b and the nuclei diameter L, has been introduced:

$$\varepsilon = \rho b L \tag{4}$$

Equation 4 allows to calculate the initial recrystallized volume fraction $F_V^{initial}(\rho, N) = \frac{4}{3}\pi N (\frac{\varepsilon}{2\rho b})^3$ as a function of N and ρ, assumed as the only free parameters in the calculation, differently from our previous approach [4] in which $F_V^{initial}$ was a third free parameter.

3. Materials and experimental procedure

The chemical composition of the AISI 316 steel studied in this paper is shown in Table I. Samples of the steel were cold rolled down to different thickness with reduction rates of 20%, 40%, 60%, 80%, 90% and then annealed in laboratory at $T = 1100$°C for different times (up to 8 min). The thermal profiles (heating and soaking) were measured and interpolated by a polynomial fitting. After electrochemical etching in a solution containing HNO_3 and HCl, samples were analysed for grain size determination through automatic image analyser. As an example, some representative micrographs are reported in Figs 1–3 relatively to the 20%, 60% and 90% deformed and annealed samples. Micro-hardness measurements were performed on the samples and related to the recrystallized volume fraction. The dislocation density ρ used as a fitting parameter in the statistical

TABLE I Chemical composition of the AISI 316 steel used in this research (mass %)

	C	Mn	Ni	Cr	Mo	Cu	Co	P
AISI 316	0.018	0.90	11.10	17.40	2.10	0.22	0.11	0.026

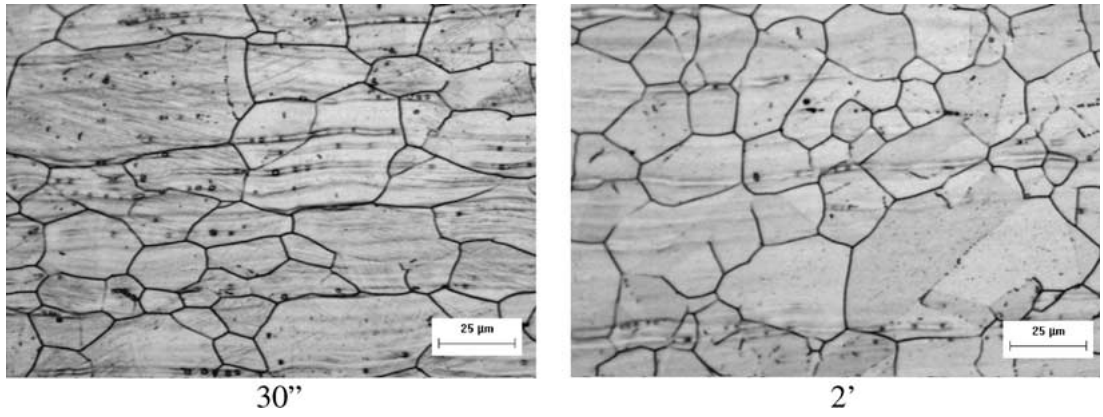

Figure 1 20% deformed 316 stainless steel annealed at 1100°C.

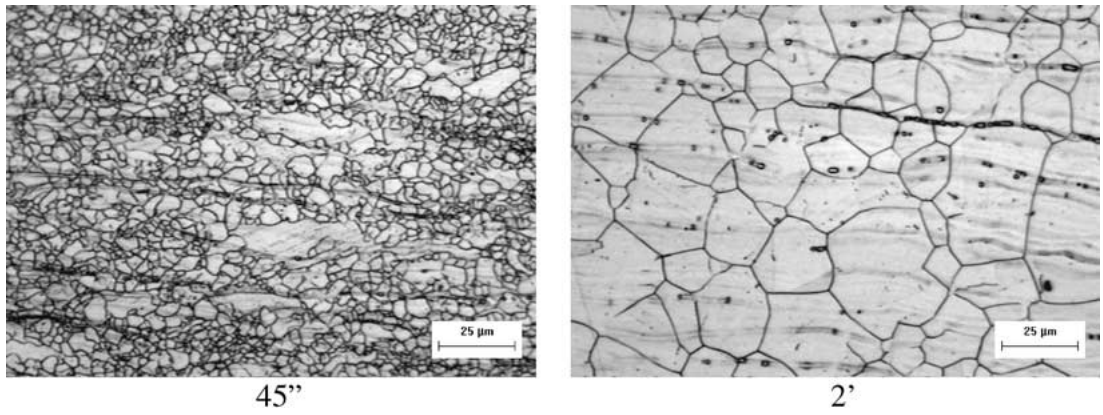

Figure 2 60% deformed 316 stainless steel annealed at 1100°C.

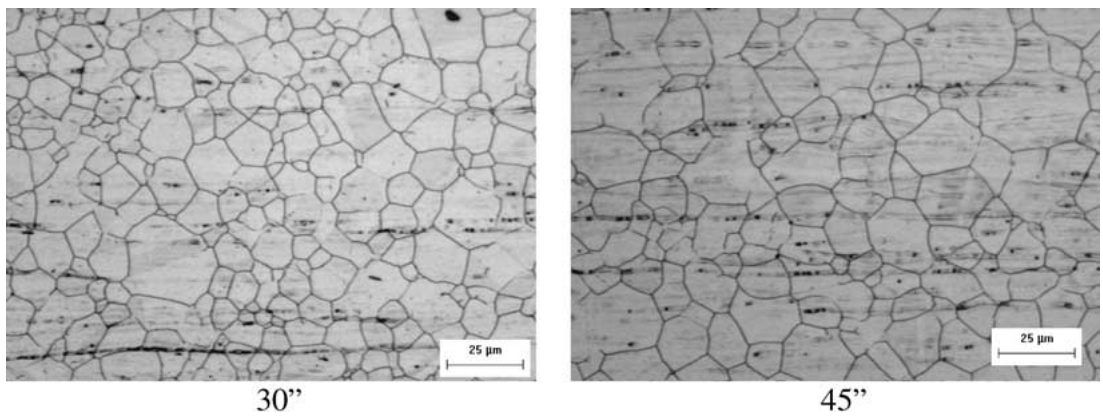

Figure 3 90% deformed 316 stainless steel annealed at 1100°C.

model was related to tensile stresses and to FWHM X-ray measurements.

4. Results and discussion

4.1. Data elaboration

After grain size determination by automatic image analysis, experimental data have been transformed in 3-D according to the Saltykov model [10] and fitted by the statistical recrystallization model. The measured heating profiles were inserted in the microstructural model to take into account the temperature dependence of boundary mobility.

Although it is common knowledge that the enthalpy (energy) of activation and especially the preexponential factor of grain boundary mobility don't usually correlate well with diffusion data, as a first approximation the mobility was calculated according to the Stokes-Einstein relationship:

$$m = \frac{D}{K_B T} = \frac{D_0}{K_B T} e^{-\frac{\Delta E}{K_B T}} \tag{5}$$

where $D =$ diffusion coefficient, $K_B =$ Boltzman constant, $\Delta E =$ activation energy of the process, $T =$ temperature. It is thus possible to take into account the effect of the annealing treatment on the material, by introducing in Equation 10 the function $T = T(t)$ from the measured heating profile. As a first approximation, in the following D was chosen to be proportional to the diffusion coefficient of Fe-γ in Fe-γ [11] and this frame D_0 was considered as a free input parameter.

The other input parameters of the model, the initial number of nuclei N and the dislocation density ρ, were considered as dependent on the cold reduction

rate and independent on the heating temperature profile, assumption based on the experimental evidence that recovery effects in an austenitic structure are negligible. From a sensitivity study of the model parameters, it came out that the shape of the initial grain size distribution is not very effective on the kinetics whereas variation of the number of nuclei N and of the dislocation density ρ are much more effective, thus suggesting a scheme for the numerical simulation according to Fig. 4.

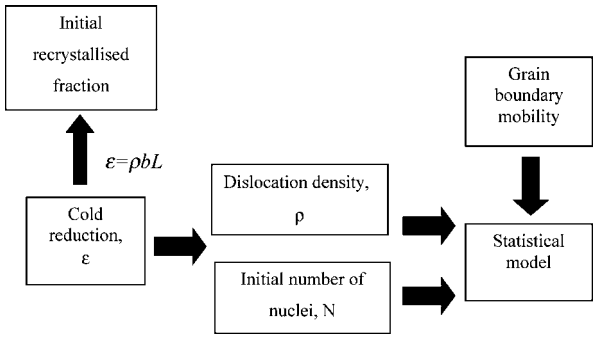

Figure 4 Simulation procedure.

4.2. Prediction of the mean radius

The experimental mean radii of samples of cold rolled AISI 316 steel at different reduction grades (20%, 40%, 60%, 80% and 90%) and annealed at different times are shown in Fig. 5 together with the values predicted by the statistical model. These results show a good agreement between the prediction of the model and experimental data. The values of the best fitting parameters used for the simulations reported in Fig. 5 are shown in Table II.

Although a smaller mean radius with a higher cold reduction should be expected, the same mean radius values have been obtained for all reduction grades. It

TABLE II Values of the best fitting parameters used for the simulations of the recrystallization and grain growth phenomena in the AISI 316 steel

Cold reduction (%)	ρ (cm^{-2})	N (cm^{-3})
20	6.0×10^{10}	2.0×10^{8}
40	1.1×10^{11}	5.0×10^{8}
60	1.5×10^{11}	7.0×10^{8}
80	2.0×10^{11}	1.0×10^{9}
90	2.2×10^{11}	1.0×10^{9}

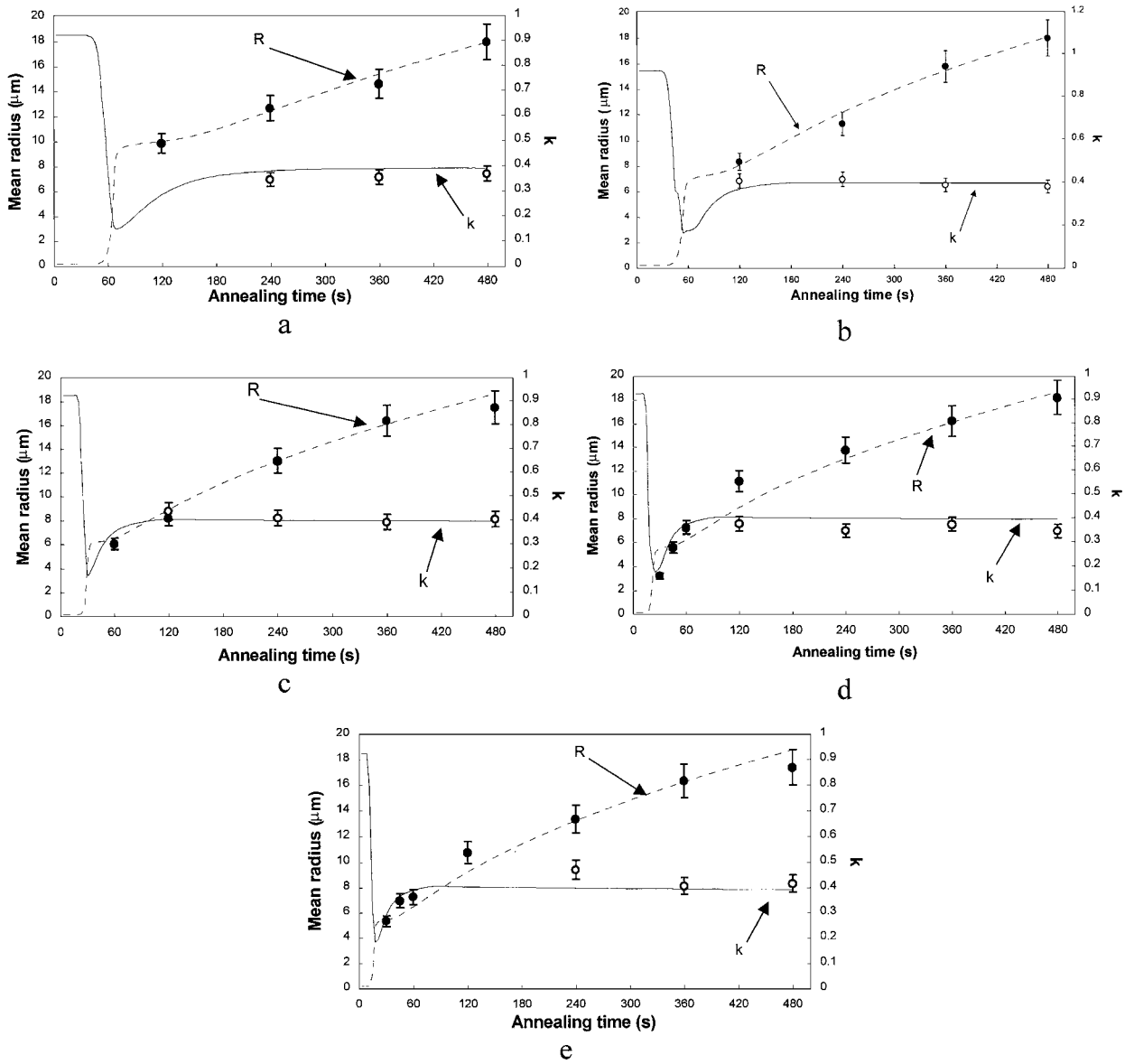

Figure 5 Experimental mean radii and variation coefficients k of samples of cold rolled AISI 316 (A: 20%, B: 40%, C: 60%, D: 80% and E: 90%) and annealed at different times in comparison with results from the statistical model.

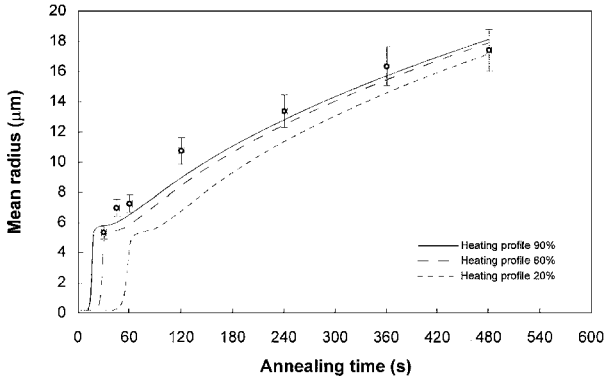

Figure 6 Influence of the different heating profiles on the grain size.

must be noted that, due to the different thickness of the samples (which come from the same hot rolled coil), the higher is the cold reduction the higher is the subsequent heating rate. Therefore, opposite effects are produced by cold reduction and by the heating rate during grain growth. In order to better analyse the effects of the heating profile on the mean radius during recrystallization and grain growth a specific set of simulations has been performed on three AISI 316 strips with different initial thickness cold rolled with the same reduction grade (90%). The results of the simulations (using the microstructural parameters $\rho = 2.2 \times 10^{11}$ cm^{-2}, $N = 1.1 \times 10^{9}$ cm^{-3}) are shown in Fig. 6 From these results it is evident that the different heating profiles, due to the thickness effect, influence significantly the grain size showing in particular the relevance of the "time" spent by the sample at the highest temperatures.

The numbers of nuclei and dislocations densities used in the calculations are shown in Fig. 7 as a function of the cold reduction grade. These results not only reflect the expected behaviour of the recrystallization and grain growth process but also represent the connection between the microstructure characteristics of the deformed material and the processing parameters. Fig. 7 is also of practical importance since, once the model has been set for a given steel, it is possible to obtain from it the parameters to simulate the behaviour of the same material subjected to different cold reduction grades.

In order to validate the dislocation density values used for the calculation, a direct dislocation density measure has been performed on the 20% deformed sample by means of Transmission Electron Microscope (TEM) according to [10]. The results are shown in Fig. 8, giving a ρ value in the sample lying in the range 4×10^{10} cm$^{-2} < \rho < 7 \times 10^{10}$ cm^{-2} to be compared with the 6×10^{10} cm^{-2} value used in the calculation.

In order to indirectly validate the dislocation density data inserted in the model as an input parameter for the higher cold deformations, the validity of the Taylor dependency between ρ and the yield strength R_{p02}, which has been found valid in polycrystalline materials [12], has been tested:

$$R_{p02} \propto \langle \rho \rangle^n \quad \text{with} \quad n = 0.5 \tag{6}$$

In Equation 6, ρ is obtained by best fitting of the experimental mean radius with the statistical model and the R_{p02} is obtained by tensile stress test. The results of this correlation are shown in Fig. 9 where a good agreement ($n = 0.54$ in comparison to the theoretical $n = 0.5$) between simulation results and Equation 6 results are obtained. This result is an indirect proof that the dislocations density ρ already identified by the model through the best fitting of the mean radius and the variation coefficient values are congruent with the experimental data R_{p02}.

As a further validation of the dislocation density values used in the calculation, X-ray diffraction measurements have been performed on the {220 planes of the deformed samples using a MoK$_\alpha$ source. Fig. 10 shows the effects of the deformation on the line shape: the higher is the deformation (and thus the dislocation density), the higher is the broadening of the diffraction peak. The validity of the following Debye-Scherrer relation usually found valid for single phase materials [13] has been tested:

$$\rho \propto \frac{1}{D^n} \tag{7a}$$

$$D = \frac{0.9 \cdot \lambda}{\cos\theta \cdot \Delta(2\vartheta)} \tag{7b}$$

The results of such validation are shown in Fig. 11. The higher value of the exponent n obtained ($n = 3.4$ in comparison to the theoretical $n = 2.0$) can be explained in terms of martensite content. In fact, Fig. 12 shows the presence of magnetic martensite (α') determining at high grades of deformation the presence of a higher dislocation density with respect to that of the single

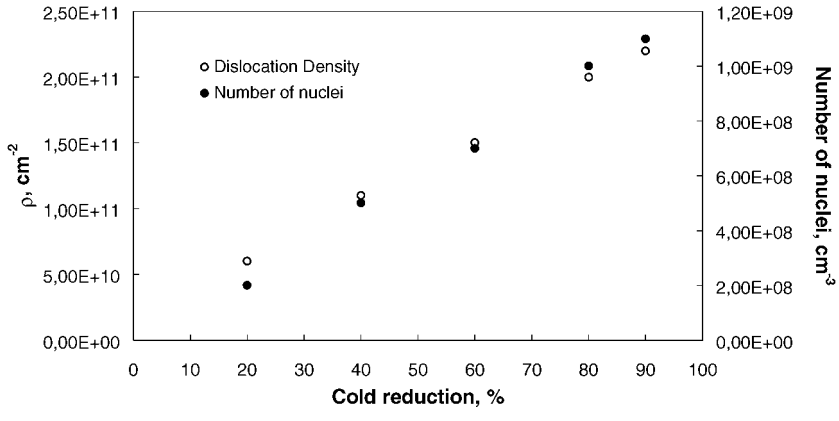

Figure 7 Calculated numbers of nuclei and dislocations densities as a function of the cold reduction grade.

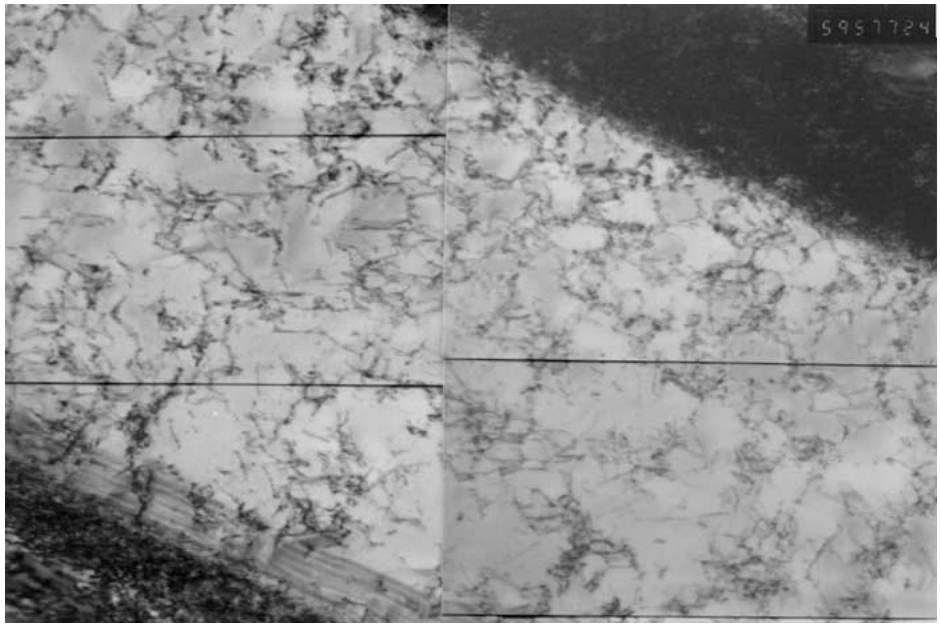

Figure 8 TEM micrograph for the 20% deformed steel.

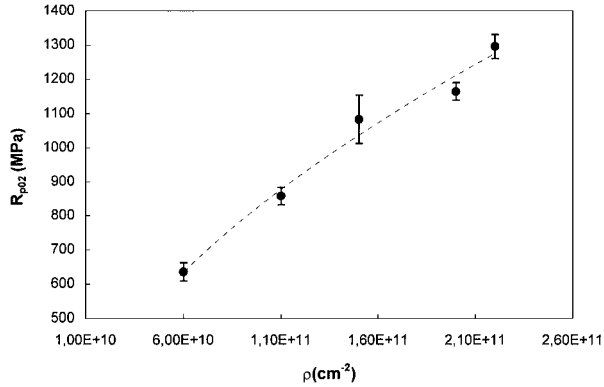

Figure 9 Validation of the Taylor dependency between ρ and the yield strength R_{p02}. The continuous line represents the best fit according to Equation 6; $R^2 = 0.98$.

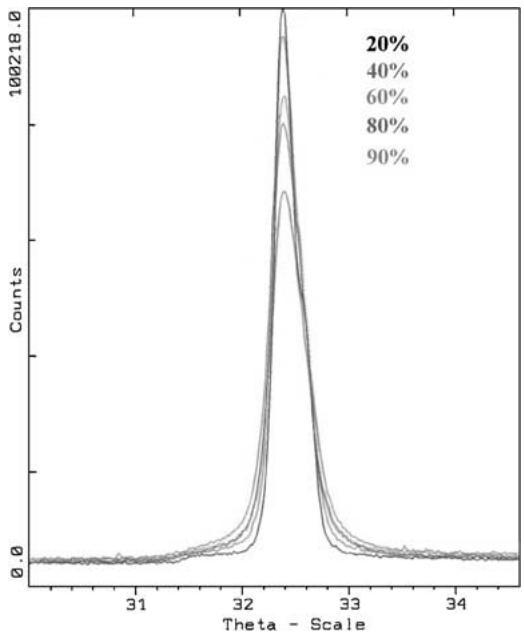

Figure 10 Effect of the deformation on the line shape of {220 X-ray diffraction peak.

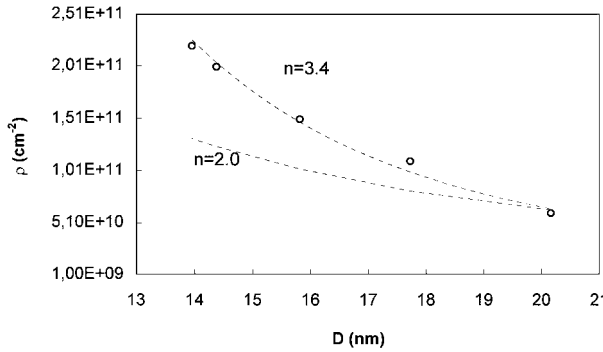

Figure 11 Validation of the Debye-Scherrer relation (Equation 7). The continuous line represents the best fit according $\rho \propto 1/Dn$ with $n = 3.4$ ($R^2 = 0.98$). The dot line represents the fit according to Equation 7.

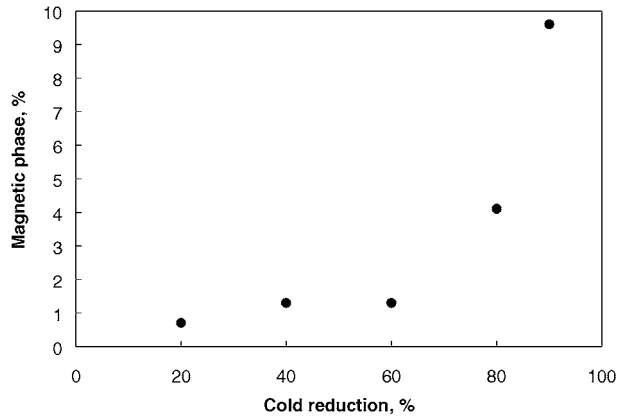

Figure 12 Magnetic phase (α'-martensite) as a function of the cold rolling grade in the AISI 316 stainless steel.

phase steel, that can lead to an increase the exponent n in Equation 7.

A comparison of the parameters used for the simulation of the AISI 316 steel with those used for the validation of the model on AISI 304 [14] is shown in Table III where m_0 is the proportional coefficient in the mobility calculation, hold constant in all the simulations. Table III shows that similar ρ and N values were

TABLE III Input parameters for recrystallization and grain growth calculations in AISI 304 and AISI 316 stainless steels

	AISI 304			AISI 316		
Cold reduction (%)	ρ (cm^{-2})	N (cm^{-3})	m_0	ρ (cm^{-2})	N (cm^{-3})	m_0
20	5.0×10^{10}	2.0×10^{8}		6.0×10^{10}	2.0×10^{8}	
40	1.2×10^{11}	3.0×10^{8}		1.1×10^{11}	5.0×10^{8}	
60	1.5×10^{11}	8.0×10^{8}	1.0×10^{-5}	1.5×10^{11}	7.0×10^{8}	3.0×10^{-6}
80	2.0×10^{11}	9.0×10^{9}		2.0×10^{11}	1.0×10^{9}	
90	2.1×10^{11}	1.2×10^{9}		2.2×10^{11}	1.0×10^{9}	

used in the calculation for both steels: A lower grain boundary mobility is found in the AISI 316 steel, due to the presence of Mo.

4.3. Prediction of the recrystallized volume fraction

Due to the general difficulty in determining the recrystallized fraction by automatic image analysis in partially recrystallized samples, a model has been developed relating the recrystallized fraction to the steel hardness [4]. This model, based on the Taylor's theory and on the assumption of a poor influence of recovery phenomena in austenitic stainless steels, lead to the following equation linking the recrystallized volume fraction at the annealing time t $F_V(t)$ to the hardness $\delta(t)$ measured at the same annealing time:

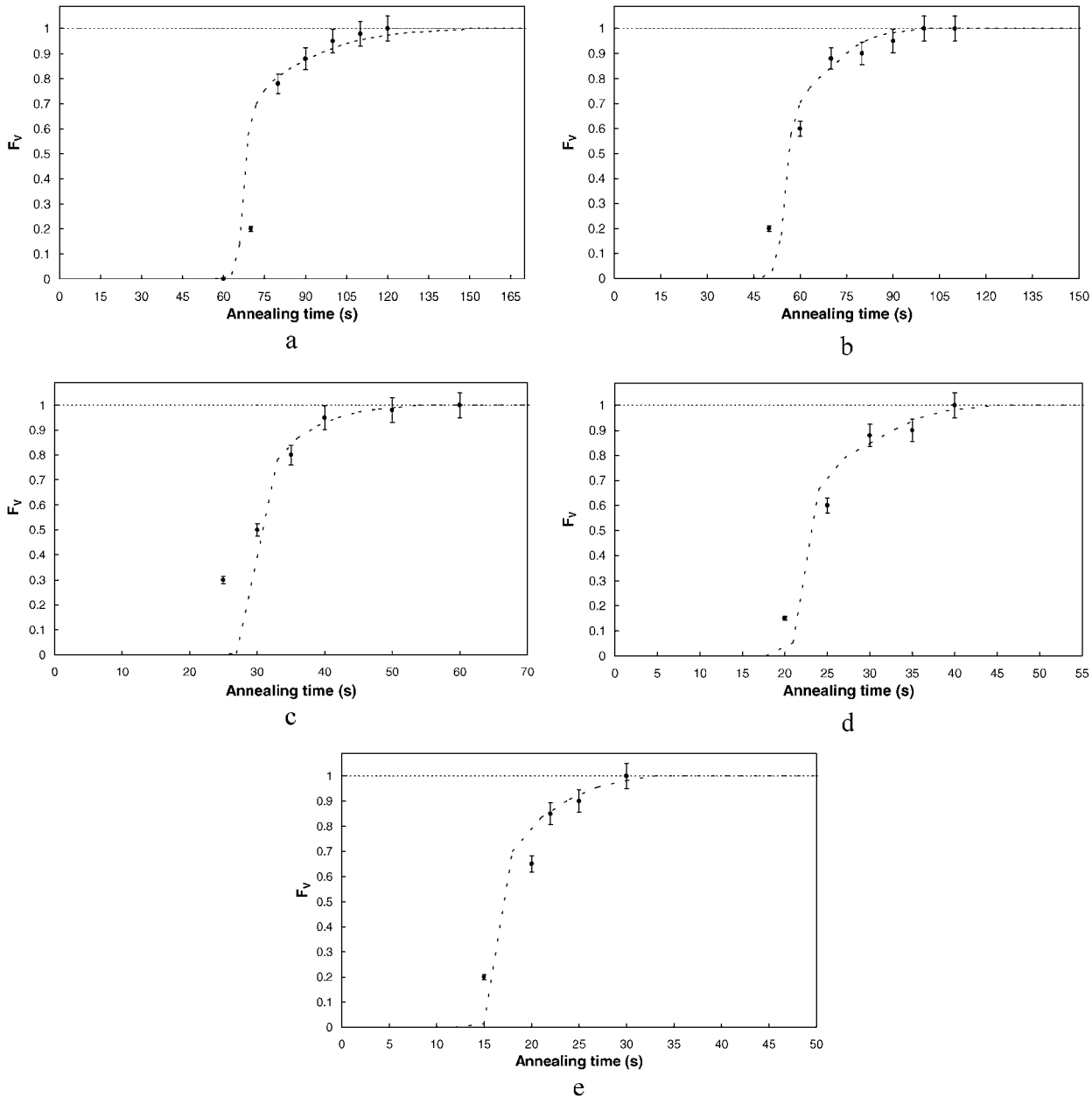

Figure 13 Comparison of the values of the recrystallized volume fraction obtained from hardness measurements and those obtained from the statistical model for the different cold reduction grades 316 (A: 20%, B: 40%, C: 60%, D: 80% and E: 90%).

TABLE IV Mean radius of samples with different reduction rates at times t_R corresponding to a complete recrystallization

Cold reduction (%)	Mean radius (μm)
20%	9.5
40%	7.8
60%	6.0
80%	5.5
90%	5.0

$$F_V(t) = \frac{\delta^2(t) - \delta_A^2}{\delta_D^2 - \delta_A^2} \tag{8}$$

where δ_D and δ_A represent the hardness in the deformed and in the completely annealed steel respectively.

The comparison of the values of the recrystallized volume fraction obtained from hardness measurements and those obtained from the statistical model is shown in Fig. 13 for the five different cold reduction grades. The good agreement obtained between indirect experimental data and model results confirms also in this case the validity of the modelling approach. In fact, the prediction of the evolution of the volume fraction by the recrystallization model (Fig. 13) should be compared with experimental data (microstructure evolution) on volume fraction. However, at the present such measures are rather difficult to be performed with reasonable accuracy and reproducibility by metallographic methods because of the insufficient definition of the obtainable microstructure images. Then, Equation 8 provides a valid alternative to more direct experimental validation of the statistical model.

From the comparison between results reported in Figs 5 and 13 it can be observed that at times corresponding to a complete recrystallization, the lower is the reduction rate the greater is the mean radius. This conclusion is in agreement with the fact that at higher cold reductions higher dislocation densities and thus higher numbers of nuclei are present in the steel with a consequent lower mean radius. These results are summarised in Table IV.

5. Conclusions

Results from a recrystallization and grain growth model based on statistical assumptions have been here discussed in comparison with measurements performed on an AISI 316 stainless steel. In particular, samples of various reduction rates of cold rolled steel were annealed at 1100°C at different times. The grain size of the samples was determined via automatic image analysis and corrected to 3-D values according to the Saltykov model. The predictions of the model (mean radius, variation coefficient and recrystallized volume fraction) are in good agreement with experimental results. As cross check of the model prediction the independent parameter "dislocation density" was found to properly correlate to the mechanical properties of the steel and to X-ray diffraction measurements. The lower grain boundary mobility found in AISI 316 with respect to that of the AISI 304 steel is attributed to the presence of Mo.

References

1. A. DI SCHINO, M. G. MECOZZI, M. BARTERI and J. M. KENNY, *J. Mat. Science* **35** (2000) 4803.
2. Y. MURATA, T. TAKEMOTO and Y. UEMATSU, in Proc. of the Int. Conf. on Stainless Steels, Chiba, June 1991, edited by ISIJ, p. 510.
3. F. J. HUMPHREYS and M. HATHERLY, "Recrystallization and related annealing phenomena" (Pergamon Oxford, 1985).
4. A. DI SCHINO, J. M. KENNY, G. ABBRUZZESE and I. SALVATORI, *J. Mat. Science* **36** (2001) 593.
5. K. W. MAHIN, K. HANSON and J. W. MORRRIS, *Acta metall.* **28** (1980) 443.
6. M. HILLERT, *ibid.* **13** (1965) 227.
7. I. SALVATORI and G. ABBRUZZESE, in 3rd International Conference on Grain Growth, Warrendale, June 1998, edited by TMS, p. 187.
8. G. ABBRUZZESE, *Acta metall.* **33** (1985) 1329.
9. G. ABBRUZZESE, I. HECKELMAN and K. LÜCKE, *ibid.* **40** (1992) 519.
10. DE HOFF and RHINES, "Quantitative Microscopy" (McGraw–Hill, New York, 1968) p. 132.
11. W. JOST, "Diffusion" (Academic Press, New York, 1960) p. 239.
12. A. S. KEH and S. WEISSMAN, "Electron Microscopy and Strength of Crystals" (Interscience, New York, 1963).
13. G. K. WILLIAMSON and R. E. SMALLMAN, *Phyl. Mag.* **1** (1956) 34.
14. A. DI SCHINO, I. SALVATORI, G. ABBRUZZESE and J. M. KENNY, in Proc. of the 5th AIMAT Conference, Spoleto, (2000) p. 533.

Received 2 August 2001
and accepted 18 July 2002